

Design of a Robotic System for MRI-Guided Deep Brain Stimulation Electrode Placement

Gregory Cole*, Julie Pilitsis† and Gregory S. Fischer*

* Worcester Polytechnic Institute, Worcester, MA, USA

† University of Massachusetts Medical School, Worcester, MA, USA

E-mail: gfisher@wpi.edu

Abstract—Deep brain stimulation (DBS) is a technique for influencing brain function through the use of implanted electrodes. Direct magnetic resonance (MR) image guidance during DBS insertion would provide many benefits; most significantly, interventional MRI can be used for planning, monitoring of tissue deformation, real-time visualization of insertion, and confirmation of placement. The accuracy of standard stereotactic insertion is limited by registration errors and brain movement during surgery. With real-time acquisition of high-resolution MR images during insertion, probe placement can be confirmed intra-operatively. Direct MR guidance has not yet taken hold because it is often confounded by a number of issues including: MR-compatibility of existing stereotactic surgery equipment and patient access in the scanner bore. The high resolution images required for neurosurgical planning and guidance require high-field MR (1.5-3T); thus, any system must be capable of working within the constraints of a closed, long-bore diagnostic magnet. Currently, no technological solution exists to assist MRI guided neurosurgical interventions in an accurate, simple, and economical manner. We present the design of a robotic assistant system that overcomes these difficulties and promises safe and reliable electrode placement in the brain inside closed high-field MRI scanners. The robot performs the insertion under real-time 3T MR image guidance. This paper describes analysis of the workspace requirements, MR compatibility evaluation, and mechanism design.

I. INTRODUCTION

Deep brain stimulation (DBS) is a technique for influencing brain function through the use of implanted electrodes. DBS is an FDA approved treatment of Parkinson's Disease and other movement disorders that has shown to be more effective than medical or surgical therapies in randomized controlled studies [1]. Studies show that DBS may have similar effects in major depression and Alzheimer's Disease [2] and other neurological disorders. Successful outcomes require accurate localization of, and guidance of the electrode to, the target intra-operatively. In typical DBS electrode insertion (Indirect MR guidance), preoperative MRI images of the brain's anatomy are acquired. A fiducial frame is then rigidly affixed to the patient, who then undergoes a computed tomography (CT) scan, where the images are spatially registered to the MR images to set the insertion trajectory. After this, it is not typical to use further radiological guidance. Because of this, most centers have adopted electrophysiological confirmation (*i.e.* micro-electrode recordings (MER)) to ensure proper intraoperative probe placement, though this step adds significantly to potential morbidity[3], and has a diminishing role in new applications/targets for DBS.

Without MER, confirmation is based on fluoroscopic images taken in the OR. These lateral images are only able

to confirm that the DBS lead is in the trajectory set by the frame. However by the time the patient enters the OR, there are a tremendous number of points where errors can be introduced: malposition of the frame requiring corrections for pitch, yaw or roll, measurement limitations, inaccuracies of the frame, targeting errors, mechanical loading effects on the frame from positioning or headstage, brain shift from CSF loss, and image fusion issues. *The use of direct MR guidance would streamline the procedure and provide a means of in-situ confirmation.*

One study examined this technique using the Nexframe (Medtronic Minneapolis, MN), which is an MR-compatible stereotactic device [4]. Mean error of this technique was 1.0mm (range 0.1mm – 1.9mm). It is felt that the majority of this error, which is comparable to indirect MR frame-based approaches, was due to the alignment of the trajectory guide that needed to be done manually, which was often difficult secondary to the confines of the bore and design of the NexFrame. *Use of a robotic alignment guide would potentially eliminate this difficulty, improve work flow, and potentially improve the accuracy of the technique.*

To date, there have been only a handful of attempts to develop MRI-compatible systems to assist interventional procedures in closed bore scanners. A thorough review of MR-compatible systems to date for image-guided interventions is presented by Tsekos, *et al.* [5]. Robotic assistance for guiding instrument placement in MRI for neurosurgery began with Masamune, *et al.* [6]. Chinzei, *et al.* [7] developed a general-purpose robotic assistant for open MRI that has been adapted for neurosurgery. A high dexterity MRI-compatible system for neurosurgery, known as the neuroArm, is presented by Sutherland, *et al.* [8].

Some developments in MRI-compatible motor technologies include Stoianovici, *et al.* who describe an MRI-compatible pneumatic stepper motor called PneuStep [9], and Dubowsky, *et al.* who presented the development of dielectric elastomer actuators (DEAs) [10]. Servo controlled pneumatic actuators have been used in the commercial Innomotion robot (Innomedic, Herxheim, Germany) and by Fischer, *et al.* [11]. Manually actuated mechanical linkages for needle guidance have been presented by Krieger, *et al.* [12]. MR-compatible haptic interfaces for fMRI by Gassert and Ganesh, *et al.* [13]. Ultrasonic Motor drive techniques that enhance MR compatibility are described by Suzuki, *et al.* [14]. The feasibility of using piezoceramic motors in MR is presented by Elhawary, *et al.* [15] and Fischer and Krieger, *et al.* [16].

The MRI robot system provides a method for performing image-guided interventions using real-time MRI images from traditional diagnostic, long-bore, high-field magnets to guide and needle insertion procedures. This is in stark contrast to much of the prior work in MRI-guided interventions, such as manual attempts by Lewin, *et al.* [17] and robotic attempts by Chinzei, *et al.* [7] that are based upon use on a low-field, open, specialized interventional magnet.

The objective of this work is to make conventional diagnostic closed high-field MRI scanners available for guiding deep brain stimulation electrode placement interventions. We employ an MRI-compatible robotic assistant for guiding DBS electrode insertion under direct, real-time MR imaging. The system is designed to allow interactive probe alignment under real-time imaging in high-field MR scanners. Use of a robotic assistant will minimize the potential for human error and mis-registration associated with the current procedure and will better address the practical issues of operating in an MR scanner bore.

II. DESIGN REQUIREMENTS

Perhaps the most daunting problem of closed bore MRI is access to the patient inside the magnet. Long bore magnets clearly require remote or compact actuation, but most presently available percutaneous needle placement robots suffer from problems that include complexity, size, and kinematic limitations. Also, importantly the instruments cannot be ferromagnetic and must not cause detrimental imaging artifacts. Unfortunately, when it comes to mobile mechanical assistants, the problem of MR compatibility aggregates and often leads to a prohibitively complex and expensive engineering entourage. Robotic assistance has been investigated for guiding instrument placement in MRI, beginning with neurosurgery [6]. Yet, there is no practical, reliable, convenient, accurate, and economical solution - this is what we intend to address with the proposed work.

A. Workspace Analysis

The workspace and working envelope are tightly constrained in the scanner bore. The bore diameter of the scanner is typically up to 60cm. With the bed in place, that leaves a clearance for the patient and robot of less than 45cm. An average skull is 20-25cm from forehead to occiput, leaving a clearance of no more than 20cm between the forehead and the top of the scanner bore. A typical stepper drive for DBS electrode placement has a travel of 50mm. In order to keep the system as generally applicable as possible, we will allow up to 100mm of insertion depth. In order to clear the skull and imaging coils, the mechanism must sweep an arc of at least 15cm radius from the target point. To enable the required range of motion for typical DBS lead placement, the robot is designed to allow 60° of motion from the sagittal plane symmetrically about the vertical. In the axial plane, the required range of motion is up to 60° from the vertical.

The robot requires a minimum of two rotations to adjust these angles and additional DOF to place the target point. Three prismatic axes, and two perpendicular rotating axis

with high precision can accomplish this task. A final resolution of 0.1 mm at the tool placement tip is supported by this. To allow for additional dexterity, an optional two additional rotations are designed into a yoke at the tip of the end effector. This end effector allows access to a volume of targets not within the original set of reachable trajectories.

B. System Requirements

The specifications for the kinematic requirements for the robot are shown in Table I. The numbered motions in the table correspond to the labeled joints in the equivalent kinematic diagram shown in Fig. 1. The first embodiment of the system for initial proof-of-concept system and Phase-1 clinical trials provide the three prismatic motions (*DOF#1 – DOF#3*), two angular motions (*DOF#4 and DOF#5*) and a manual cannula guide (*DOF#6*) as shown in Fig. 1. Two additional optional DOF are incorporated into the yoke at the end of the mechanism; these allow for repositioning of the target point to enhance the usable workspace. In future designs, automated needle insertion may be implemented to allow complete “closed-loop” control of the insertion procedure based on real-time MR imaging.

In the traditional procedure using a stereotactic frame, a set of x , y and z coordinates are dialed in to set the tip position and a set of θ_1 and θ_2 align the orientation of the electrode cannula about that tip location. To mimic that functionality, a remote center of motion (RCM) mechanism is employed; this is equivalent to aligning the motion axes of *DOF#4 – DOF#6* such that they intersect at the target location. Since significant changes in orientation are clinically inadvisable in neurological interventions, the RCM point is set at the target point rather than the insertion point typically used [18]. If it becomes necessary to rotate about the entry point (*i.e.* burr hole), techniques such as the “virtual RCM” described by Boctor and Webster, *et al.* may be employed [19].

TABLE I
KINEMATIC SPECIFICATIONS FOR ROBOT

	Degree of Freedom	Motion	Requirements
1)	<i>Axial motion</i>	0 – 300mm	Servo Control
2)	<i>Horizontal Motion</i>	0 – 100mm	Servo control
3)	<i>Vertical Motion</i>	±50mm	Servo and manual control
4)	<i>Axial Plane Angle</i>	-60° – 0°	Servo control
5)	<i>Sagittal Plane Angle</i>	±30°	Servo control
6)	<i>Cannula Insertion</i>	100mm	Manual or Automated

The accuracy of the individual servo-controlled joints is targeted to be the encoder resolution of 0.01mm, and the needle placement accuracy of the robotic system itself is targeted to be 0.1mm in free space. The actual accuracy of the complete system is expected to be somewhat less when registration errors and mechanical deflection are introduced. A target accuracy of better than 1.0mm approximates the voxel size of the MR images used which represents the finest possible targeting precision. The clinically significant target is typically 1mm in size.

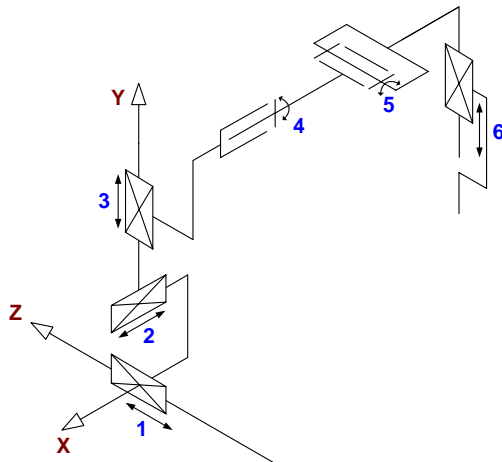


Fig. 1. Equivalent kinematic diagram of the robot - details the primary six degrees of freedom for needle insertion procedures with this manipulator.

C. MRI Compatibility Requirements

The requirements for MR compatibility of robotic systems include: MR safety, maintained image quality, and ability to operate unaffected by the scanner's electric and magnetic fields. Ferromagnetic materials must be avoided entirely, though non-ferrous metals such as aluminum, brass, nitinol and titanium, or high strength plastic and composite materials are permissible. However, the use of any conductive materials in the vicinity of the scanner's isocenter must be limited because of the potential for induced eddy currents to disrupt the magnetic field homogeneity. To prevent or limit local heating in the proximity of the patient's body, the materials and structures used must be of carefully chosen geometry to avoid eddy currents and resonance. In this robot, all electrical and metallic components are isolated from the patient's body. All linkages are made out of high strength, biocompatible plastics including Ultem and PEEK.

III. SYSTEM AND COMPONENT DESIGN

A. System Architecture

The mechanism design is capable of positioning the electrode under remote control of the physician without moving the patient out of the imaging space. This enables the use of real-time imaging for precise placement of needles in soft tissues. In addition to structural images, protocols for diffusion imaging and MR spectroscopy are available intraoperatively, promising enhanced visualization and targeting of pathologies. Accurate and robust needle placement devices, navigated based on such image guidance, are becoming valuable clinical tools and have clear applications in several other organ systems.

The architecture of this system is modeled after that of an MRI-guided robotic system that we have developed for prostatic interventions[11], and is presented in Fig. 2. Planning (*i.e.* localization of the subthalamic nucleus (STN) and identification of a safe trajectory) is performed on pre-procedure MR images or pre-operative images registered to the intra-operative images. Additionally, multi-parametric image datasets and statistical atlases may be visualized. The

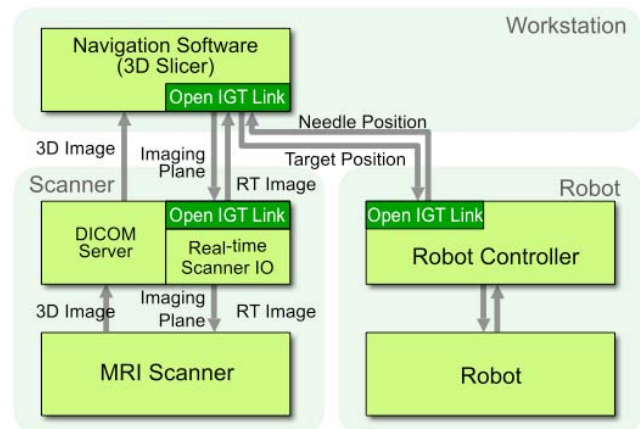


Fig. 2. System architecture for robotic neurosurgical electrode implantation interventions using the developed system as described by Tokuda *et al* [20].

needle trajectories required to reach these desired targets are evaluated here, subject to anatomical constraints, as well as constraints of the needle placement mechanism.

During the procedure, the robot is localized via a fiducial marker tube aligned with the cannula insertion axis that is imaged in multiple robot configurations. Since the robot base is fixed in scanner coordinates, this registration is only necessary once. Intraoperatively, MR images are acquired showing the target location and cannula axis. An iterative process of imaging and robot motion allow alignment of the needle axis through the target while the patient is positioned within the magnet bore. Alignment is confirmed with MR images along the cannula axis showing the fiducial tube and target location. Once alignment is achieved, the electrode cannula is inserted manually under real-time MR image guidance.

B. Mechanism Design

The robotic manipulator must operate with high precision, and utilize actuation systems that can be finely controlled, with minimal backlash while maintaining MR compatibility. In addition to this, jerk when the appendage makes its initial movement from a standstill must be minimized.

A thorough description of manipulators commonly used in medical robots is presented by Taylor and Stoianovici [21]. There are two primary styles of linkages and actuators: 1) Highly rigid linkages with no back drive potential (*e.g.* [21]), and 2) compliant linkages which will allow resistive forces of the tissues to be transmitted back to the user (*e.g.* [22]). The relative virtues of both are widely debated; however, in this application the machine will operate on delicate brain tissue and it is far more important to position the tools precisely than to be able to use feedback from the device. Further, in the event of a power failure or an emergency stop, it is imperative that the tool remains locked in its current position.

Many surgical robots that manipulate laparoscopic tools, needles or other shafts through a single point of entry employ a remote center of motion ([21]), as it allows up to four-DOF around the RCM point: three rotational and one translational (depth). A mechanically constrained RCM mechanism was selected for this system; however, it is developed with the

additional limitation of operating in a very small volume in the presence of strong magnetic and electric fields. To accommodate this, a parallelogram linkage was used. This was selected instead of a double sliding beam linkage or a pivoted arm robot because it does not suffer from large wear surfaces, or high velocities that reduce precision associated with these designs. In addition, by using a parallelogram linkage, an armature with a vertical profile of 40mm and a horizontal profile of 60mm has been achieved, leaving a large amount of working volume left within the scanner bore for the surgeon to operate, as shown in Fig. 3.

Sterility has been taken into consideration for the design of the end effectors. In particular, the portions of the manipulator that contact the cannula will be removable and made of materials that are suitable for sterilization. The remainder of the robot will be draped.

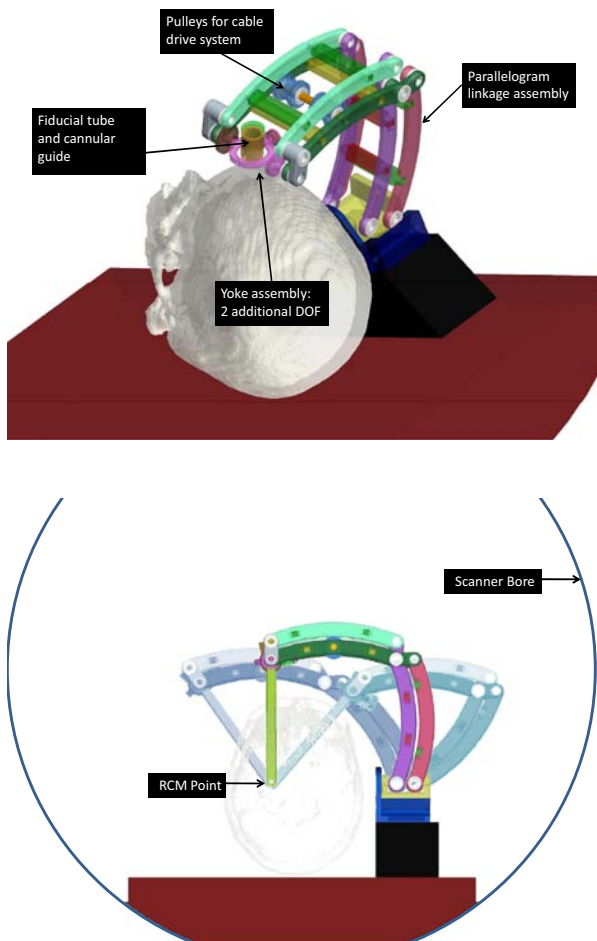


Fig. 3. Mechanism design for remote center of motion appendage, the rod end indicates the RCM point. Both primary rotations and the two optional rotations at the yoke are cable driven from the base of the manipulator.

C. Sensor and Actuator Selection

We first investigated commercially available actuation options. An experimental evaluation of the following three different MRI-compatible actuators was performed: the Shinsei rotary ultrasonic motor, the Nanomotion linear ultrasonic motor and a pneumatic cylinder actuator [16]. The effect of these actuators on the signal-to-noise ratio (SNR) of MRI

images was compared under a variety of experimental conditions. Evaluation was performed with the controller inside and outside the scanner room and with both 1.5T and 3T MR scanners. A comparison of the motors' compatibility in the different configurations is described using four popular MRI sequences for diagnostic, real-time and functional imaging. In order to ensure scanner-independence, it is not possible to rely on the penetration panel due to variations in the built-in filtering and connector availability.

Experience demonstrates the advantages of placing the controller inside the scanner room and communication through a fiber optic medium. SNR loss is reduced by placing an MR-compatible controller inside the scanner room.

An alternative piezoelectric motor from Piezomotor was selected for use in this robot. With proper output filtering and sufficient shielding on the motor driver housing, SNR is limited to 3% [23]. In addition to this, torque and speed performance of the motor allowed for a direct drive coupling which eliminated many sources of inaccuracies caused by wear and backlash of power transmission systems.



Fig. 4. The current state of the armature prototype. The main linkage arm provides 2-DOF RCM motion, along with a yoke that provides 2-DOF added dexterity as necessary, and is to be mounted on a 3-DOF prismatic base. The mechanism design, cable drive system, and piezoelectric motor location is shown.

Many traditional position sensing modalities are not practical for use in an MR environment. However, there are two methods that do appear to have potential: optical encoders and direct MR image guidance. Standard optical encoders (EM1-1250 linear and E5D-1250 rotary encoder modules with PC5 differential line drivers - US Digital, Vancouver, Washington) are used in this robotic system. The encoders are placed on the joint actuators and reside in the scanner bore. The differential signal driver sits on the encoder module, and the signals are transmitted through shielded, twisted pairs cables to the encoder interface. The encoder

interface is a shielded circuit board that is fixed near the robot base and routes the signals to the front face of the robot control enclosure. Inside of the shielded controller enclosure are differential line receiver modules that translate the signals back to standard TTL levels and feeds them into an FPGA module.

The encoders have been incorporated into the robotic device and perform without any evidence of stray or missed counts. The encoders have been thoroughly tested in a 3T MRI scanner for functionality and induced effects in the form of imaging artifacts as described in [11]. Direct MR image guidance is described in Section III-E. It may be used for high-level visual servo control and image-based verification of the procedure, but the sample rate is not fast enough to allow for closed-loop servo control of the joints.

D. Robot Controller Hardware

MRI is very sensitive to electrical signals passing in and out of the scanner room. Electrical signals passing through the patch panel or wave guide can act as antennas, bringing stray RF noise into the scanner room. As determined MR compatibility experiments presented in [16], the robot controller is placed inside of the scanner room with no external electrical connections.

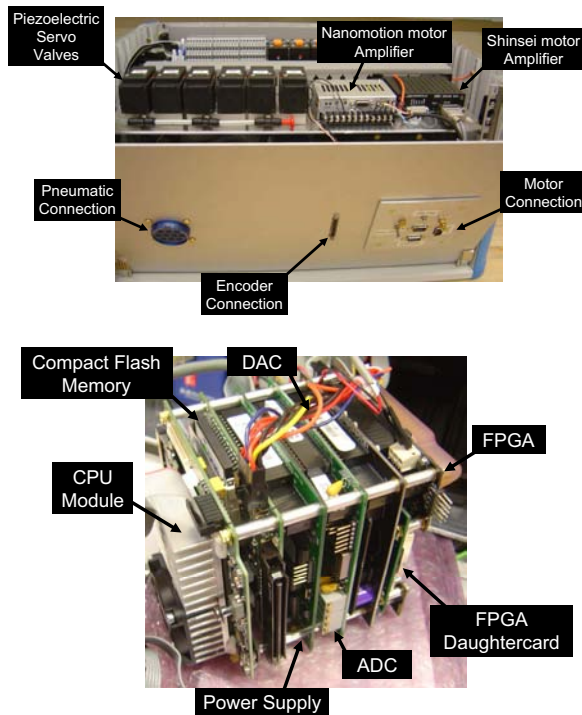


Fig. 5. The controller (top) is shown in the configuration for comparing actuation techniques, supporting two types of piezoelectric motor amplifiers and piezoelectric pneumatic servo valves. It contains the embedded Linux PC on a PC-104 stack (bottom) providing low-level servo control. The EMI shielded enclosure is placed inside the scanner room near the foot of the bed.

The controller comprises an electro-magnetic interference (EMI) shielded enclosure that sits at the foot of the scanner bed; the controller has proved to be able to operate 3m from the edge of 1.5T and 3T scanner bores. A view of the controller enclosure with the cover removed is shown in Fig. 5 (top). Inside of the enclosure is an embedded computer as

shown in Fig. 5 (bottom). The controller computer system is a 4" x 4" PC-104 form factor and includes: Cheetah EPM-32p, (Versalogic Corp., Eugene, OR), power regulation and field programmable gate array (FPGA), brake valve control, and general I/O (HE104-75W and FPGA-104 respectively, (Tri-M Systems, Port Coquitlam, BC, Canada), and analog outputs for valve or motor control and analog inputs for pressure and force sensor input (RMM-1612 and DMM-16-AT respectively, Diamond Systems, Mountain View, CA). Also in the enclosure are the custom low noise amplifiers for the piezoelectric motors that we have developed. Due to the complexity and power required to effectively drive piezoelectric motors, and the high cost and purpose specific design of commercially available piezomotor drivers, we have developed a set of driver boards based on the PIC32 MCU so that they are easy and cost effective to implement.

Control software on the embedded PC, provides for low-level joint control and an interface to interactive scripting and higher level trajectory planning. The software implemented on the embedded Linux computer is based upon the CISST open source software library [24]. Communication between the low-level control PC and the planning and control workstation sitting in the MR console room is through a 100-FX (100Mbps) fiber optic Ethernet connection (B&B Electronics, EIR-M-ST Industrial Media Converter, Ottawa, IL). Power is supplied to the controller from 48V shielded, linear DC power supply that resides inside the scanner room. No electrical connections pass out of the scanner room (only fiber optic communications), thus significantly limiting MR imaging interference.

E. Interface Software

The user interface for the robot is based on 3D Slicer open-source surgical navigation software [25]. The navigation software runs on a Linux-based workstation in the scanner's console room. A customized graphical user interface (GUI) specially designed for robotic DBS electrode placement is in development. OpenIGT Link, an open-source device connection and communication tool developed for image-guided therapy, is used to exchange various types of data including control commands, position data, and images among the components as shown in Fig. 2 and described in more detail in [26].

In the planning phase, pre-operative images are retrieved from a DICOM server and loaded into the navigation software. Registration is performed between the pre-operative planning images and intra-operative imaging. Target points and trajectories for the electrode insertion are selected according to the pre-operative imaging. Once the patient and robot are placed in the MRI scanner, a small stack of MR images is acquired near the expected robot location with the robot orientation set to its centered, home position. Four additional image sets are acquired corresponding to the robot orientation set at its extremes. These image sets will capture a large Z frame fiducial marker affixed to the base of the robotic system that can be used to determine the exact position and orientation of the linkage as demonstrated by

DiMaio *et al.* [27]. Also, in each of the five image sets, the vector along the length of the fiducial tube coaxial with the electrode cannula is extracted. The intersection of these vectors lies at the RCM point, whose location is determined from a pivot calibration. Also extracted is the orientation of the axis of rotation for each axis. The x , y , and z axis alignment is known approximately since the robot is fixed to the head frame. Since image feedback is used to set the target point, resolving the exact axis alignment is not required. After the registration phase, the robot can accept target coordinates represented in the image (patient) coordinate system in standard Right-Anterior-Superior (RAS) coordinates. In the current system, the electrode and cannula are inserted manually along the robotically aligned guide. Needle advancement in the tissue can be visualized in two complementary ways: 1) a 3D view of robot end effector model combined with pre-operative 3D image re-sliced in planes intersecting the insertion axis, and 2) 2D real-time MR images acquired from the planes along or perpendicular to the needle path. The interface software enables “closed-loop” needle guidance, where the action made by the robot is captured by the MR imaging, and immediately fed back to a physician to aid their decision for the next action. The reason for keeping a human in the loop is to increase safety and allow for the live MR images to monitor progress. The robot fully aligns the cannula guide before any contact is made with the patient. If necessary, the placement is adjusted responsive to the MR images.

IV. VALIDATION

The validation plan for the system has two components. The first is evaluation of the robotic system’s inherent accuracy. This is to be performed using independent measurements of the robot’s motions; individual axes will be evaluated with a digital dial gauge and the full system by an optical tracking system. The next stage is evaluation of the integrated system; this includes the robotic system, registration of robot to scanner, planning software, and scanner integration in addition to MR compatibility.

A two-stage insertion procedure will be used, with introduction of a guide sheath (cannula) for the DBS electrode as the first stage, followed by placement of the DBS electrode through the sheath in the second stage.

DBS lead accuracy will be performed using previously published methods [4]. Specifically, a gelatin-filled synthetic skull phantom containing eight separate targets that are 9-10 cm away from the skull surface will be used. The guide sheath will be placed through the tool holder and will be used to access targets ipsilateral to its mounting position. Imaging requirements include the identification of the target and entry point, which together define the desired trajectory, and efficient feedback to the interventionalist during targeting and electrode insertion. The targets in the phantom study are identifiable cylindrical slots measuring 3mm in diameter.

Alignment of the tool holder will be confirmed using two rapid orthogonal T2-weighted images (confirmation scan: 2D-TSE, FOV = 250mm, matrix = 256 256, slice thickness

= 2mm, No. of slices = 3, TR/TE = 96/2000ms, flip angle = 90, turbo factor = 24, SAR = 1.4 W/kg, time = 18 s) along the desired trajectory orientation. For the purpose of accuracy assessment, these confirmation scans are only used to screen for gross errors in trajectory alignment. The high resolution 3D volume acquisition will be repeated following insertion of the sheath to assess its position relative to the target. Positional errors perpendicular to the desired trajectory (radial error) at target depth will be tabulated. The entire imaging procedure will be performed for each of these eight targets (four per side) and repeated on two separate occasions, producing 16 measures of lead placement accuracy.

V. RESULTS

The primary focus of this work is to detail the design process for the robotic system. The first step in this process is a thorough workspace analysis including both mechanical and anatomical constraints. The mechanism design presented here has been meticulously evaluated to ensure compatibility with the DBS electrode placement procedure in traditional closed-bore MR scanners. Design and analysis are complete, material selection has been finalized, the MR compatibility of the actuators has been verified and the controller evaluated. The robot is in the process of being constructed. Incorporating all of the discussed specification, designs, and design limitations, we have constructed most of the the unactuated prototype shown in Fig. 3. It is conceivable that the robot takes a change of form after initial prototypes are built and tested. We expect to begin validation experiments shortly.

VI. CONCLUSIONS AND FUTURE WORKS

We have designed an MRI-compatible manipulator and the support system architecture that can be used for electrode placement in the brain. The robot has been designed such that it will operate in the confined space between the patient’s skull and the scanner bore in a high-field, closed bore MRI scanners. The configuration allows the use of diagnostic MRI scanners in interventional procedures; there is no need for open or large bore scanners that often are difficult to come by and sacrifice image quality. Initial evaluation of the system’s workspace, MR-compatibility, workflow, and user interface has been very positive. All of the primary elements of the system are now in place; further refinement of the control system and interface software are in progress.

The next phase of this work focusses on completing construction of the current prototype system, performing further MR compatibility trials, and validating the system with the method described above. As can be seen in Fig. 4 a significant portion of the prototype linkage has been constructed, and so far mechanical properties are promising. Upon satisfactory results, we will perform cadaver trials in preparation for developing a refined clinical-grade system for Phase-1 clinical trials. The initial application will be DBS electrode placement in the STN for treatment of Parkinson’s disease. However, the real benefit of the system will be to evaluate DBS as a treatment choice for other neurological

diseases. For depression treatment, in particular, MER is not viable and image guidance is the only way to reliably reach the required placement accuracy. The robot, controller and/or system architecture are generally applicable to other MR robotic applications as demonstrated by the extension of our work in MR-guided prostate interventions.

As diagnostic MRI is becoming more and more affordable, simple and robust needle placement mechanisms may facilitate a wide array of diagnostic and therapeutic interventions in the brain and in other organ systems. Robotic assistance may also reduce variability among practitioners and speed up their learning curve. Robotic systems may also serve as validation tools for researchers whose work requires precise targeting of anatomical regions identified by MR imaging. Moreover, these devices are identically usable with any tomographic imaging modality: MRI, CT, PET, SPECT, and any combination of thereof.

ACKNOWLEDGMENTS

The authors would like to thank our collaborators at the Johns Hopkins University including Iulian Iordachita and Axel Krieger, along with Yi Wang for help with the MR compatibility evaluation, and at the Brigham and Women's Hospital including Noby Hata and Junichi Tokuda for help in navigation software development, and Nathan Rosenblad for his help developing the piezoelectric motor driver boards.

REFERENCES

- [1] G. Deuschl and et al., "Neurostimulation for parkinsons disease.," *JAMA*, vol. 301, pp. 104–105, Jan 2009.
- [2] B. Aouizerate and et al., "Deep brain stimulation for ocd and major depression.," *Am J Psychiatry*, vol. 162, p. 2192, Nov 2005.
- [3] P. A. Starr, C. W. Christine, P. V. Theodosopoulos, N. Lindsey, D. Byrd, A. Mosley, and W. J. Marks, "Implantation of deep brain stimulators into the subthalamic nucleus: technical approach and magnetic resonance imaging-verified lead locations.," *J Neurosurg*, vol. 97, pp. 370–387, Aug 2002.
- [4] A. J. Martin, P. S. Larson, J. L. Ostrem, W. K. Sootsman, P. Talke, O. M. Weber, N. Levesque, J. Myers, and P. A. Starr, "Placement of deep brain stimulator electrodes using real-time high-field interventional magnetic resonance imaging.," *Magn Reson Med*, vol. 54, pp. 1107–1114, Nov 2005.
- [5] N. V. Tsekos, A. Khanicheh, E. Christoforou, and C. Mavroidis, "Magnetic resonance-compatible robotic and mechatronics systems for image-guided interventions and rehabilitation: a review study.," *Annu Rev Biomed Eng*, vol. 9, pp. 351–387, 2007.
- [6] K. Masamune, E. Kobayashi, Y. Masutani, M. Suzuki, T. Dohi, H. Iseki, and K. Takakura, "Development of an mri-compatible needle insertion manipulator for stereotactic neurosurgery.," *J Image Guid Surg*, vol. 1, no. 4, pp. 242–248, 1995.
- [7] K. Chinzei, N. Hata, F. A. Jolesz, and R. Kikinis, "Mri compatible surgical assist robot: System integration and preliminary feasibility study.," in *MICCAI*, vol. 1935, pp. 921–930, October 2000.
- [8] G. R. Sutherland, I. Latour, A. D. Greer, T. Fielding, G. Feil, and P. Newhook, "An image-guided magnetic resonance-compatible surgical robot.," *Neurosurgery*, vol. 62, pp. 286–92; discussion 292–3, Feb 2008.
- [9] D. Stoianovici, "Multi-imager compatible actuation principles in surgical robotics.," *Int J Med Robot*, vol. 1, pp. 86–100, Jan 2005.
- [10] K. Tadakuma, L. DeVita, S. Y., and S. Dubowsky, "The experimental study of a precision parallel manipulator with binary actuation: With application to mri cancer treatment.," in *Proc. IEEE International Conference on Robotics and Automation ICRA '08*, pp. 2503–2508, May 21–May 23, 2008.
- [11] G. S. Fischer, I. I. Iordachita, C. Csoma, J. Tokuda, S. P. DiMaio, C. M. Tempny, N. Hata, and G. Fichtinger, "Mri-compatible pneumatic robot for transperineal prostate needle placement.," *IEEE/ASME Transactions on Mechatronics*, vol. 13, June 2008.
- [12] A. Krieger, R. C. Susil, C. Mnard, J. A. Coleman, G. Fichtinger, E. Atalar, and L. L. Whitcomb, "Design of a novel mri compatible manipulator for image guided prostate interventions.," *IEEE Trans Biomed Eng*, vol. 52, pp. 306–313, Feb 2005.
- [13] R. Gassert, N. Vanello, D. Chapuis, V. Hartwig, E. Scilingo, A. Bicchi, L. Landini, E. Burdet, and H. Bleuler, "Active mechatronic interface for haptic perception studies with functional magnetic resonance imaging: compatibility and design criteria.," in *Proc. IEEE International Conference on Robotics and Automation ICRA 2006* (N. Vanello, ed.), pp. 3832–3837, 2006.
- [14] T. Suzuki, H. Liao, E. Kobayashi, and I. Sakuma, "Ultrasonic motor driving method for emi-free image in mr image-guided surgical robotic system.," in *Proc. IEEE/RSJ International Conference on Intelligent Robots and Systems IROS 2007*, pp. 522–527, Oct. 29 2007–Nov. 2 2007.
- [15] H. Elhawary, A. Zivanovic, M. Rea, B. Davies, C. Besant, D. McRobbie, N. de Souza, I. Young, and M. Lamprth, "The feasibility of mr-image guided prostate biopsy using piezoceramic motors inside or near to the magnet isocentre.," *Med Image Comput Comput Assist Interv Int Conf Med Image Comput Comput Assist Interv*, vol. 9, no. Pt 1, pp. 519–526, 2006.
- [16] G. S. Fischer, A. Krieger, I. I. Iordachita, C. Csoma, L. L. Whitcomb, and G. Fichtinger, "Mri compatibility of robot actuation techniques – a comparative study.," *Int Conf Med Image Comput Comput Assist Interv*, Sept. 2008.
- [17] J. S. Lewin, A. Metzger, and W. R. Selman, "Intraoperative magnetic resonance image guidance in neurosurgery.," *J Magn Reson Imaging*, vol. 12, pp. 512–524, Oct 2000.
- [18] R. Taylor, J. Funda, B. Eldridge, S. Gomory, K. Gruben, D. LaRose, M. Talamini, L. Kavoussi, and J. Anderson, "A telerobotic assistant for laparoscopic surgery.," *IEEE Engineering in Medicine and Biology*, vol. 14, no. 3, pp. 279–288, 1995.
- [19] E. M. Boctor, R. J. Webster, H. Mathieu, A. M. Okamura, and G. Fichtinger, "Virtual remote center of motion control for needle placement robots.," *Comput Aided Surg*, vol. 9, no. 5, pp. 175–183, 2004.
- [20] J. Tokuda, S. P. DiMaio, G. S. Fischer, C. Csoma, D. Gobbi, G. Fichtinger, N. Hata, and C. M. Tempny, "Real-time mr imaging controlled by transperineal needle placement device for mri-guided prostate biopsy and brachytherapy.," *Proc. of the 16th Meeting of the International Society for Magnetic Resonance in Medicine - ISMRM*, p. 3004, May 2008. <http://www.ismrm.org/08/EP1.htm>.
- [21] R. H. Taylor and D. Stoianovici, "Medical robotics in computer-integrated surgery.," *IEEE Trans RA*, vol. 19, pp. 765–781, Oct. 2003.
- [22] P. Abolmaesumi, S. Salcudean, W.-H. Zhu, M. Sirospour, and S. DiMaio, "Image-guided control of a robot for medical ultrasound.," vol. 18, pp. 11–23, Feb. 2002.
- [23] Y. Wang, G. Fischer, C. Sotak, and G. Fischer, "Optimization of piezoelectric motors to enhance mr compatibility for interventional devices.," *17th Scientific Meeting and Exhibition of the International Society of Magnetic Resonance in Medicine*, April 2009.
- [24] A. Kapoor, A. Deguet, and P. Kazanzides, "Software components and frameworks for medical robot control.," in *Proc. IEEE International Conference on Robotics and Automation ICRA 2006* (A. Deguet, ed.), pp. 3813–3818, 2006.
- [25] N. Hata, S. Piper, F. A. Jolesz, C. M. C. Tempny, P. M. Black, S. Morikawa, H. Iseki, M. Hashizume, and R. Kikinis, "Application of open source image guided therapy software in mr-guided therapies.," *Med Image Comput Comput Assist Interv Int Conf Med Image Comput Comput Assist Interv*, vol. 10, no. Pt 1, pp. 491–498, 2007.
- [26] J. Tokuda, G. S. Fischer, C. Csoma, S. P. DiMaio, D. G. Gobbi, G. Fichtinger, C. M. Tempny, and N. Hata, "Software strategy for robotic transperineal prostate therapy in closed-bore mri.," *Int Conf Med Image Comput Comput Assist Interv*, Sept. 2008.
- [27] S. P. DiMaio, E. Samset, G. S. Fischer, I. I. Iordachita, G. Fichtinger, F. Jolesz, and C. M. Tempny, "Dynamic mri scan plane control for passive tracking of instruments and devices.," *Med Image Comput Comput Assist Interv Int Conf Med Image Comput Comput Assist Interv*, vol. 10, no. Pt 2, pp. 50–58, 2007.